Simulation of Flow Across a Spacer Grid with RANS and LES Turbulence Models

Giacomo Busco, Yassin A. Hassan

Department of Nuclear Engineering, Texas A&M University, 3133 TAMU, College Station, TX 77801, USA

INTRODUCTION

The highly turbulent flow structure of the coolant in the region downstream of the spacer grid of a pressurized water reactor (PWR) is particularly challenging to model using traditional computational fluid dynamics (CFD) techniques. The failure of the classic two-equations RANS models is mainly due to the not-isotropic turbulent flow structure in the region downstream the spacer grid, which has been addressed experimentally by Nguyen and Hassan (2017). Spacer grids with mixing vanes have received considerable attention among the nuclear engineering community, particularly those involved in CFD simulations. Different benchmark studies have been carried out in the past. The round robin benchmark exercise is an example. It was carried out against the New Experimental Studies of Thermal-Hydraulics of Rod Bundles (NESTOR) experimental runs for a 5×5 rod bundle with split-type mixing vane grids, considering both isothermal and non-isothermal cases (Kang & Hassan, 2016).

The typical high Reynolds number flow inside a nuclear reactor core, present a large spectrum of turbulent time and length scales. Direct numerical resolution of the Navier-Stokes equations using direct numerical simulation (DNS) techniques is practically impossible due to the limitations of computational resources. Turbulence modeling plays a key role in reducing the high computational cost associated with such high Reynolds number flow conditions.

We will compare some of the turbulent flow field characteristics in the region downstream the mixing vanes using large eddies simulation (LES) model and RANS two-equation standard Wilcox k-omega model. The Reynolds number ($Re = 14{,}000$) for the present set of simulations was relatively low if compared with the normal operating conditions of typical PWR reactors. We used CD-Adapco™ STAR-CCM+ commercial CFD code as the main investigation tool.

Turbulence models

LES model

We selected the wall-adapting local eddy viscosity (WALE) subgrid stress closure model in this study (Nicoud & Ducros, 1999). This model is based on the square of the velocity gradient tensors, accounting for the effect of the strain tensor S_{ij} and rotation rate tensor Ω_{ij} of the smallest turbulent fluctuations. The closure of the eddy viscosity is expressed in algebraic form as in many LES closures:

$$v_t = (C_w \Delta)^2 \frac{(S_{ij}^d S_{ij}^d)^{\frac{3}{2}}}{(\overline{S_{ij}}\,\overline{S_{ij}})^{\frac{5}{2}} + (S_{ij}^d S_{ij}^d)^{\frac{5}{4}}} \quad (1)$$

It shall be noted that the closure relation takes into account the rotational part of the velocity tensor gradient, which provides physical insight into the flow where secondary flow is the dominant part of the problem. Filtering is not required in building the eddy viscosity model, contrary to the classical Smagorinsky method, since only the filtered local flow quantities are needed. (Nicoud & Ducros, 1999).

RANS Wilcox k-omega model

The standard Wilcox k-omega model (Wilcox, 1993) has been selected in order to have a better resolution in the wall region, especially for the spacer grid region. The model use the standard Boussinesq approximation to close the set of RANS equations:

$$v_t = \frac{k}{\omega} \quad (2)$$

For both LES and k-omega the low-y^+ wall treatment has been used.

Geometry and Mesh

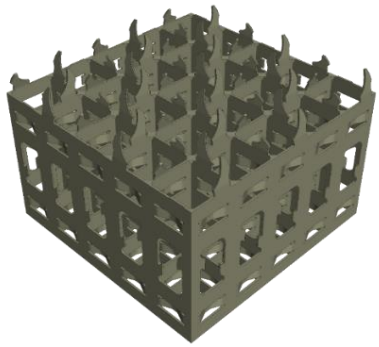

Fig. 1: spacer grid with split-type mixing vanes geometry.

The test case is a scaled PWR fuel rod bundle with a 5×5 lattice. All of the dimensions such as the bundle pitch (12.6 mm), rod diameter (9.5 mm), and spacer grid features (dimples, springs, and mixing vanes) are identical to the full

scale 17×17 lattice fuel rod bundle. The only difference is the 5×5 lattice arrangement versus the 17×17 lattice arrangement. Figure 1 shows the model of the spacer grid with split-type mixing vanes.

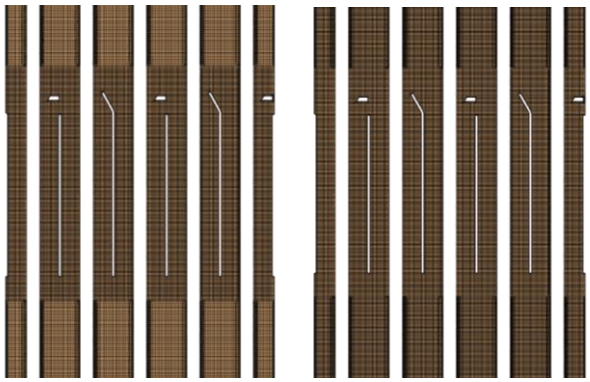

Fig. 2: mesh grid details. RANS (left). LES (right).

An unstructured trimmed mesh was created due to the highly complex geometry of the fuel rod bundle with dimples, springs, and mixing vanes. The hexahedral mesh structure was kept as homogeneous as possible in order to ensure that most of the computational domain was covered with a predominant structured-like mesh. Two computational meshes were tested (Figure 2): the first mesh with 25 million cells, mainly for the RANS model and a 100 million mesh for the LES model case.

RESULTS

Vertical Planes Results

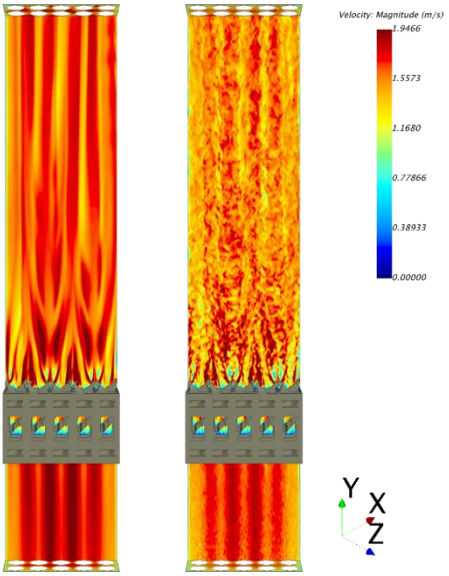

Fig. 3: Instantaneous velocity field. RANS (left) LES (right)

Figure 3 shows the instantaneous velocity profile for both models LES (right) and RANS (left). The low Reynolds number flow of the simulations gave, as expected, comparable results in terms of local time averaged velocity profiles. The turbulent statistics of such flow conditions did not influence the models closure relation of both models. Figure 4 shows the time averaged velocity profiles components for both LES and RANS. The second order statistics, variance of the turbulent flow velocity components (diagonal terms of the Reynolds stress tensor) shows a complete different behavior. The LES model tends to produce less diffusive profiles than RANS. LES variance velocity peaks tends to be more resolved than RANS.

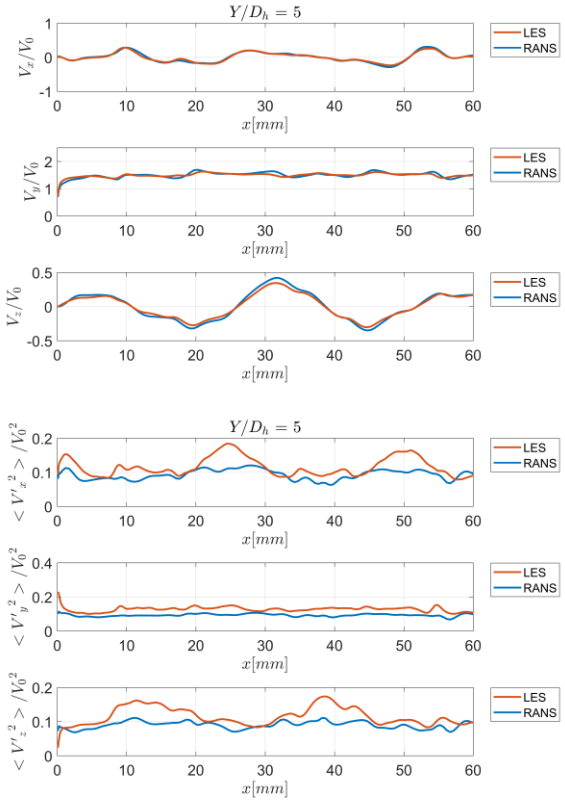

Fig. 4: Time averaged velocity components profiles (top). Velocity variance components profiles (bottom)

Horizontal Planes Results

One of the effects caused by the presence of the split-type vanes at the top of the spacer grid is to generate an intense inter-channel mixing. This will increase the heat transfer efficiency downstream the spacer grid region.

To investigate the secondary induced flow structure, we evaluated the secondary flow intensity (SFI) defined as:

$$SFI = \frac{1}{A}\sum_i \frac{A_i\sqrt{{V_x}^2 + {V_z}^2}}{\bar{V}_y} \quad (8)$$

This parameter gives the area-averaged ratio between the in-plane magnitude of the two spanwise velocity components $V_{hor} = \sqrt{V_x{}^2 + V_z{}^2}$ and the mean streamwise velocity component $\overline{V}_y$.

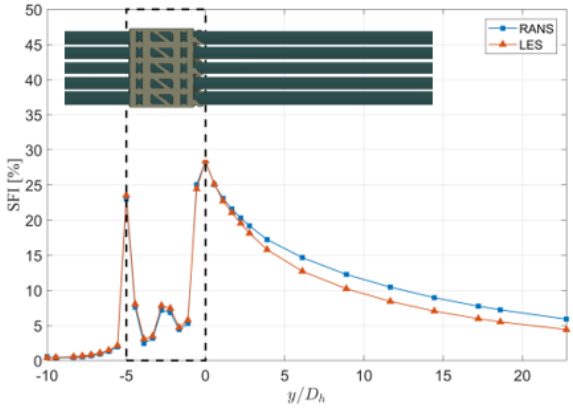

Fig. 5: Secondary flow intensity across the spacer grid.

As noted in Figure 5, there are three distinctive peaks: the first peak is due to the bottom of the spacer grid presence whereas the second peak is due to the presence of the springs and dimples at the spacer grid/bundle interface. The third peak (which also has the highest magnitude) is due to the presence of the split-type mixing vanes at the top of the spacer grid. It can be seen that the RANS model gives the same peaks magnitudes but a slower decay rate, if compared to LES model.

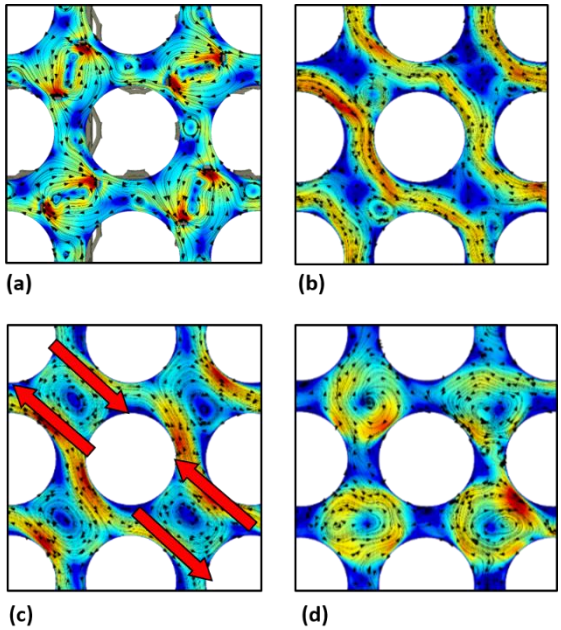

Fig. 6: Secondary flow structure. y/Dh = 1 (a). y/Dh = 3 (b). y/Dh = 5 (c). y/Dh = 10 (d).

Figure 6 shows the structure of the secondary flow at different elevations obtained from the LES model. It is evident from analysis of the secondary flow downstream of the spacer grid that there are three types of flow behavior. In the region immediately after the mixing vanes, two energetic small vortex structures, rotating in opposite direction, are generated in the middle of each sub-channel by two adjacent vanes, as shown in Figure 5a. These rotating vortex structures induce shear forces (as indicated by the red arrows in Figure 5c) at the vortex/flow interface, which accelerates the surrounding fluid and promotes cross flow in the fuel rod bundle. The rotating vortex structures become larger and less energetic as they transfer their momentum to the surrounding flow (Figure 5d) and these vortex structures eventually merge to form a single vortex, which decreases the secondary flow intensity.

CONCLUSIONS

In this study we have compared two types of turbulence modelling approach: linear eddy viscosity model (k-omega RANS) and scale resolving simulations (LES) for the spacer grid with mixing vanes geometry. The low Reynolds number flow physics did not influence the local time averages velocity profiles. Second order statistics, such as variance of the velocity components profiles, showed relevant differences. Secondary flows intensity was found to be the same in the region upstream the spacer grid, but with a different, slower decay for the RANS model. More physical insight was given about the secondary cross flow structure induced by the split-type mixing vanes.

REFERENCES

1. Kang, S. K., & Hassan, Y. A. Computational fluid dynamics (CFD) round robin benchmark for a pressurized water reactor (PWR) rod bundle. Nuclear Engineering and Design, 301, 204–231. (2016).

2. Nguyen, T., & Hassan, Y. Stereoscopic particle image velocimetry measurements of flow in a rod bundle with a spacer grid and mixing vanes at a low Reynolds number. International Journal of Heat and Fluid Flow, 67, 202–219. (2017).

3. Nicoud, F., & Ducros, F. (1999). Subgrid-scale stress modelling based on the square of the velocity gradient tensor. *Flow, Turbulence and Combustion*, *62*(3), 183–200.

4. David C. Wilcox. Turbulence Modeling for CFD. DCW Industries. (2006).